OPEN ACCESS Freely available online

PLoS one

Neural Correlates of Visual Motion Prediction

Daniel Cheong[1,2], Jon-Kar Zubieta[2,3,4], Jing Liu[2,3]*

1 Department of Biostatistics, University of Michigan, Ann Arbor, Michigan, United States of America, **2** Molecular and Behavioral Neuroscience Institute, University of Michigan, Ann Arbor, Michigan, United States of America, **3** Department of Psychiatry, University of Michigan, Ann Arbor, Michigan, United States of America, **4** Department of Radiology, University of Michigan, Ann Arbor, Michigan, United States of America

Abstract

Predicting the trajectories of moving objects in our surroundings is important for many life scenarios, such as driving, walking, reaching, hunting and combat. We determined human subjects' performance and task-related brain activity in a motion trajectory prediction task. The task required spatial and motion working memory as well as the ability to extrapolate motion information in time to predict future object locations. We showed that the neural circuits associated with motion prediction included frontal, parietal and insular cortex, as well as the thalamus and the visual cortex. Interestingly, deactivation of many of these regions seemed to be more closely related to task performance. The differential activity during motion prediction vs. direct observation was also correlated with task performance. The neural networks involved in our visual motion prediction task are significantly different from those that underlie visual motion memory and imagery. Our results set the stage for the examination of the effects of deficiencies in these networks, such as those caused by aging and mental disorders, on visual motion prediction and its consequences on mobility related daily activities.

Citation: Cheong D, Zubieta J-K, Liu J (2012) Neural Correlates of Visual Motion Prediction. PLoS ONE 7(6): e39854. doi:10.1371/journal.pone.0039854

Editor: Michelle Hampson, Yale University, United States of America

Received January 17, 2012; **Accepted** May 28, 2012; **Published** June 29, 2012

Funding: The authors have no support or funding to report.

Competing Interests: The authors have declared that no competing interests exist.

* E-mail: ljing@umich.edu

Introduction

The ability to mentally keep track and predict motion trajectories of moving objects is important in many human activities, such as driving, walking on the street, reaching, or taking aim at enemies in battles. For example, it is known that drivers' mistakes in the extrapolation of other vehicles' motion contribute to automobile accidents [1]. The brain substrates of motion trajectory prediction and the influence of their functions on human subject performance have not been systematically examined. In this study, we quantitatively measured human subjects' performance in a motion trajectory prediction task, and examined task-related brain activity modulation with functional magnetic resonance imaging (fMRI) in an event-related design.

We hypothesized that many brain regions, including but also beyond the visual cortex, would be involved in such a task, and therefore examined whole brain activity modulation. It is clear from previous studies that motion information processing without direct perception involves a large number of brain regions far beyond the visual cortex. Multiple frontal and parietal regions are implicated in motion working memory [2,3,4,5]; mental rotation [6,7,8,9]; and multiple object tracking, a task in which subjects keep track of a subset of multiple moving objects [10,11,12]. Parietal and frontal regions, as well as the anterior cingulate, insula and basal ganglia, have also been associated with visual motion imagery [13,14,15]. The superior parietal lobule has been particularly implicated in the generation of mental images (and in multiple object tracking) [12,16,17,18]. The visual cortex is also an integral part of motion processing in the absence of direct perception. The middle temporal area (MT) and V3a in the human extrastriate visual cortex are particularly responsive to motion [19,20,21,22,23]. Human MT activity correlates with the direction of moving stimuli and perceptual decisions [24]. Perturbation of MT and V3a activity also disrupts speed and direction perception [25,26,27,28,29]. Similarly, single MT neurons in non-human primates are selective for stimuli direction and speed and systematic alteration of MT activity alters their motion perception [30,31,32,33,34,35,36,37]. MT is also activated during visual motion memory and imagery [2,5,6,14,15,38,39,40,41].

In this study, we examined both task-related activation and deactivation. Sensory processing involves not only the activation of certain brain regions, but also the deactivation of others. Two major types of deactivation: the deactivation of the default mode network (DMN) and cross-modal deactivation, have been reported in the literature. Visual perception, memory and imagery have been shown to be associated with task-induced deactivation of many brain regions, some of which belong to the DMN, which consists of a number of (largely) midline frontal, parietal and temporal regions [42,43,44,45] (but also see [46]). Cross-modal deactivation, which is the deactivation of sensory cortices of other modalities such as auditory and somatosensory, has also been reported during visual perception and imagery [47,48,49,50]. Therefore, it would be of importance to understand the role of both regional activations and deactivations.

Materials and Methods

Ethics Statement

All participants signed an informed consent after an explanation of the experimental protocol and addressing questions from participants, as approved by the University of Michigan Institutional Review Board.

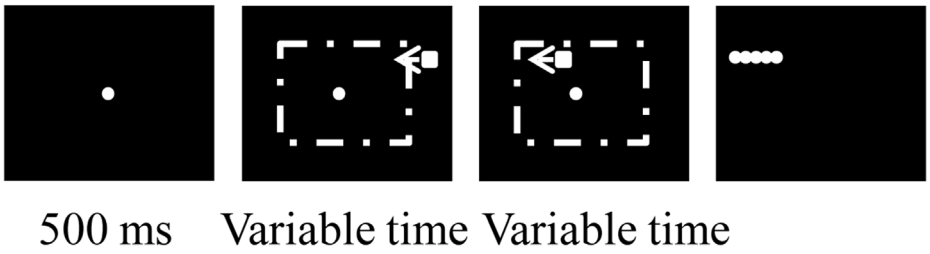

Figure 1. Task design (''Prediction'' trials). Each trial started with the appearance of the FP. After 0.5 s, a square appeared near the edge of the screen and moved across the screen at a constant direction and speed. An invisible occluder was at the center of the screen (the rectangle with the dashed line), and the square disappeared from view as it encountered the occluder. Subjects were instructed to assume that the square kept moving behind the occluder. After 2 to 4 sec., the FP turned off and five targets appeared. Subjects pressed appropriate buttons to indicate which target was closest to the final position of the square. In ''perception'' trials, no occluder was present and the square was visible throughout the trial.
doi:10.1371/journal.pone.0039854.g001

Participants

7 female and 5 male healthy subjects between the ages 24 and 52 (mean = 36.4) participated in the study. Volunteers were screened for the presence of medical and psychiatric disease and substance abuse. Subjects also had normal or corrected-to-normal vision. Upon examining the behavioral data, we determined that one male subject's performance was at chance level (see below), and the data from this subject was thus excluded from further analyses.

Experimental Setup and Data Acquisition

Whole-brain blood-oxygen-level-dependent (BOLD) signal was acquired using a 3.0 Tesla GE Signa system (Milwaukee, WI) and a standard radio frequency coil. A T2*-weighted sequence was used with the following parameters: single-shot combined spiral in/out acquisition [51], gradient echo, repetition time (TR) = 2 s, echo time (TE) = 30 ms, flip angle = 90°, field-of-view (FOV) = 20 cm, matrix size = 64×64, slice thickness = 3 mm with no gap. 30 axial slices were taken. The duration of the functional scan matched the duration of the task. Anatomical scans for the purpose of cortical area localization were performed with a T1-weighted high-resolution sequence: 3-dimentional spoiled gradient recalled echo (3-DSPGR), TR = 25 ms, minimum TE, FOV = 24 cm, matrix size = 256×256, slice thickness = 1.4 mm. Visual stimuli were presented using the integrated functional imaging system (Psychology Software Tools, Inc., Pittsburg, PA). Subjects viewed visual stimuli using Nordic Neurolab goggles, which allow SVGA display in stereo vision. Motor responses were recorded through a fiberoptic response collection device. We used foam pads around the head along with a forehead strap to minimize subjects' head movement in the scanner.

Motion Trajectory Prediction Task

Subjects performed the task inside the MR scanner with an *event-related* design (Figure 1). Each trial started with a fixation point (FP) appearing at the center of the visual display and staying on throughout the trial. Subjects were instructed to keep fixation until the FP disappeared, in order to minimize the use of smooth eye pursuit in our task. Half of the trials were randomly chosen as the ''perception'' trials. In these trials, a small, white square (0.75 deg in length) appeared 500 ms after the fixation spot onset, at a random location on the screen with a horizontal distance of between 10 to 15 degrees from the FP. It moved to the opposite side of the monitor at a constant direction and speed. The direction, therefore, was left or right. The speed was either 3 or 6 deg/sec, and both the direction and the speed were pseudo-randomly interleaved from trial to trial. The square disappeared together with the FP after a variable time of 2 to 4 seconds. Simultaneously with the disappearance of the square and the FP, five white, equi-distance target dots appeared (0.5 deg in diameter) in a horizontal line on the path of the square. Subjects pressed one of five buttons on the response pad to indicate which target corresponded to the final location of the square. We jittered the positions of the five targets to ensure that each target would be selected with an equal probability across all trials. In the other half of the trials (the ''prediction'' trials), the square became invisible after a variable time between 333 ms to 2.33 s when it went behind an invisible occluder (centered on the display, 16 deg in length), but subjects were instructed that the square still moved at the same direction and speed. The square (invisible for part of the duration) also traveled a variable 2 to 4 seconds before the end of the trial, at which point the five targets appeared and the FP disappeared. The subjects again pressed one of five buttons to indicate the final location of the square. The intertrial interval was variable and between 1.5 and 4.5 seconds so as to allow enough reaction time for the subjects. Each session was 7 minutes long and contained a variable number of trials because of the variable trial duration. Each subject performed 5 to 7 sessions. The subjects were not given feedback about the accuracy of their performance.

Data Analysis (Behavioral Responses)

We computed the average error rate and reaction time for perception and prediction trials separately in each session that each subject participated in. In each trial, if the subject chose the correct target, the error was defined as 0. If the subject chose a target that was next to the correct target, the error was 1; and so on. Note that random choices would not generate an average error rate of 2 (for five targets), because the error rate depended on where the correct target was. For example, if the leftmost target was correct, random choices would render an average error rate of 2; but if the center target was correct, random choices would render an average error rate of 1.2. An average reaction time was computed as the time between target onset and the manual response.

Data Analysis (fMRI Data Analysis)

fMRI data underwent standard preprocessing. Ten seconds of data at the beginning of each session was discarded to allow scanner saturation. Images were slice time corrected, realigned and smoothed with SPM2 using a 5 mm Gausian filter (Wellcome Institute of Cognitive Neurology, London, UK). Subsequent analyses were performed with SPM2. A General Linear Model was constructed with the perception trials and prediction trials across all sessions as trial types and the movement parameters

collected during scans as regressors, and a canonical HRF function was applied to the event-related trial structure (with the trial duration = 0 in SPM). The onset of each trial (as entered in the SPM models) was the onset of the moving square. We computed the linear contrasts of 1) prediction trials alone; 2) perception trials alone; 3) prediction vs perception trials; and 4) perception vs. prediction trials. The contrast *t*-maps of individual subjects were coregistered with the T1 anatomical images, and normalized with the Montreal Neurological Institute (MNI) template. We examined the contrast images at the group level and regions that showed task-induced activation or deactivation were defined as those that included at least 10 voxels with $p<0.01$ after False Discovery Rate (FDR) correction for multiple comparisons, adjusting for the size of the cluster under consideration. In this model, the prediction trials had two components, a brief period when the square was visible, and a longer period when it was occluded. To verify that the brain activity in these trials was not mainly driven by the visible period and that the extent of deactivation was not affected by our model selection, we built an alternative model using the time when the square went behind the occluder as the onset of the prediction trials. The results that we obtained from these two models were qualitatively very similar (data not shown).

Data Analysis (Regions of Interest)

The activated and deactivated brain regions identified in the main contrasts were used to define Regions of Interest (ROI), which were then extracted using the *Marsbar* toolbox in SPM [52]. The main analysis with these ROIs was their correlation with task performance. For each subject and each ROI in each session, we obtained an average beta value for each trial type (perception and prediction) as the approximation of the level of modulation. We then computed the correlation between the modulation and the average error rate of each subject with the Spearman rank correlation test [53]. Error rates in the prediction trials were used in most of the correlation calculations because our study focus was on motion prediction. The error rates in the perception trials were used to calculate correlations with the differential activation of "Perception" – "Prediction" trials. We performed a "permutation test with ranks" to control for false positives in multiple testing [54]. In this test, we randomly assigned each error rate to a subject in each permutation while keeping the ROI data intact (label swapping). We then computed and ranked correlation coefficients for the permuted data. After 10,000 permutations, we built null distributions for each rank (e.g. the highest correlation coefficient in each permutation was used to build the null distribution for the highest correlation coefficient that we observed in the actual data). We then computed p values of the observed correlation coefficients against their own null distribution. The analyses were conducted in Matlab (Mathworks, Inc., Natick, MA, USA) unless otherwise noted.

Results

Task Performance

The mean error rate was 0.63 ± 0.05 (ste) for the perception trials, 0.83 ± 0.08 (ste) for the prediction trials. The error rates were lower in the perception than in the prediction trials for all but one subject, significant for the group (paired t test, $p = 0.001$). The reaction time was not different in prediction and perception trials (perception: 1.19 ± 0.03 sec; prediction: 1.18 ± 0.04 sec. t test, $p = 0.5$). This is consistent with our instruction to the subjects that they should mentally track the trajectory of the occluded object instead of using alternative strategies such as estimating time lapse to infer the final position of the object. No difference in performance was observed between trials with speed = 3 deg/sec and 6 deg/sec (paired t test. For error rates in prediction trials, $p = 0.17$; for error rates in perception trials, $p = 0.66$). Therefore, trials with different speeds were combined in subsequent analyses.

Group Analysis of Task-related Activation and Deactivation

The most robust activation, during both prediction and perception trials, is bilateral hippocampus (Table 1 and Figure 2). This is consistent with the role of the hippocampus in spatial navigation and memory. The only other region that showed task-related activation was the orbital frontal cortex (Brodmann Area, or BA, 11) during perception trials.

Interestingly, we observed wide-spread *deactivation* in both conditions (Table 1 and Figure 2), including the thalamus, the caudate nucleus, the insula, the cingulate and paracingulate cortex, the inferior parietal gyrus and superior temporal gyrus. In addition, inferior frontal gyrus and precuneus showed deactivation in perception trials; whereas precentral gyrus showed deactivation during prediction trials.

Group Analysis of Differential Activity in Perception and Prediction Conditions

Table 2 and Figure 3A show the brain regions with greater activity during prediction trials, compared to perception trials. These included the anterior cingulate (BA32), the lingual gyrus, the region between the inferior frontal gyrus and precentral gyrus (most likely BA 44), the middle temporal gyrus (BA 39), bilateral inferior parietal lobule (BA 40), and bilateral anterior insula. Note that some of these regions showed deactivation in both conditions, and their differential activity indicates less deactivation in prediction trials; some other regions did not show significant activation or deactivation in either conditions but showed differential activity when the two conditions were contrasted.

Table 2 and Figure 3B show the regions with greater activity during perception compared to prediction. These included mostly the bilateral extrastriate visual cortex in the middle occipital gyrus, likely incorporating MT as well as V3a [19,23,25,55]. In addition, the right cingulate cortex (BA31) also showed higher activity in perception trials. Again, we did not find significant activation/deactivation of the extrastriate visual cortex in perception or prediction trials (more in Discussions) even though these regions showed differential activity when the two conditions were contrasted.

Correlation of ROI Activity and Task performance

Table 3 and Figure 4 show a summary of the correlations between error rates and the extracted ROI modulations. Whereas regions that showed activation during either perception or prediction did not show a consistent pattern of correlation with error rates, the deactivated regions showed a uniform trend of negative correlation with error rates (chi-square test, $p<0.002$), even though few showed individually significant correlation after correcting for multiple testing. In other words, the more deactivated these regions are, the lower the error rates.

Examining the correlation between error rates and regions that showed differential activity in the two trial conditions, we found a trend of negative correlation between error rates and most ROIs that were differentially activated in either perception or prediction trials (Table 3 and Figure 4). This group effect achieved statistical significance against the null hypothesis that, at chance, equal

Table 1. Summary of brain activation during prediction and perception trials, with the likely Brodmann Areas indicated in the parentheses.

Region (BA)	Volumn (# voxels)	peak coord (x, y, z, MNI)	Peak T	P	% mod. Mean (ste)
Perception, activation:					
R. hippocampus	3305	34, −28, −10	12.08	<0.001	0.98 (0.15)
L. hippocampus	2995	−28, −22, −12	9.20	<0.001	0.85 (0.12)
Orbital frontal cortex (11)	297	6, 58, −10	6.55	0.037	1.05 (0.22)
Perception, deactivation:					
L. Thalamus	508	−10, −16, 0	10.53	<0.001	0.72 (0.07)
R. Inferior frontal gyrus (44)	3378	54, 16, 28	9.60	<0.001	1.28 (0.13)
Precuneus/median cingulated/paracingulate gyri (7, 24)	5008	−4, −42, 56	9.52	<0.001	1.38 (0.16)
R. thalamus	365	16, −22, 12	9.37	0.001	0.82 (0.10)
L. insula	402	−34, 18, 8	6.59	<0.001	1.04 (0.17)
Caudate nucleus	229	14, 4, 8	6.17	0.011	0.78 (0.13)
L. superior temporal gyrus (42)	181	−50, −30, 18	5.66	0.038	1.27 (0.24)
L. Inferior parietal lobule (40)	175	−36, −56, 44	5.45	0.044	1.08 (0.17)
Prediction, Activation:					
L. hippocampus	1318	−30, −26, −4	9.45	<0.001	1.06 (0.15)
R. hippocampus	1589	28, −22, −16	8.36	<0.001	0.86 (0.13)
Prediction, Deactivation:					
Median cingulate and paracingulate gyri (7, 24)	4213	0, −2, 46	11.13	<0.001	1.19 (0.14)
R. precentral gyrus (6), inferior parietal gyrus (40)	2803	62, 6, 22	8.96	<0.001	1.27 (0.14)
R. thalamus	267	18, −24, 10	8.82	0.004	0.77 (0.11)
Caudate nucleus	163	−14, 10, 6	7.05	0.059	0.71 (0.15)
L. thalamus	168	−6, −22, 0	6.96	0.052	0.56 (0.07)
L. insula	227	−44, −4, 10	5.63	0.011	0.89 (0.15)
L. superior temporal gyrus (42)	234	−50, −28, 18	5.34	0.009	1.27 (0.23)

Peak coord: peak coordinates; p: corrected p value; % mod: % modulation.
doi:10.1371/journal.pone.0039854.t001

numbers of ROIs should show positive and negative correlations (chi-square test, $p = 0.02$).

Discussion

In this study we measured the performance of human subjects in a motion trajectory perception and prediction task and determined task-related brain activity. We have shown that a number of brain regions were activated or deactivated during the task, and that a number of brain regions exhibited differential activity when two task conditions were contrasted. We have also shown that the activity of some of these regions, individually or as a group, was correlated with task performance. Our results provide initial information on the brain network involved in motion trajectory prediction and pave the way for future studies on how this process is affected when the sensory and cognitive systems are challenged and how it influences human performance in scenarios such as driving, reaching and aiming.

The main task-related activation was observed in the hippocampus and this is consistent with its role in working memory, especially spatial memory, spatial orientation and navigation [56,57,58,59]. Deactivation was observed in a widespread network of cortical and subcortical regions, and is consistent with previous studies in which deactivation has been reported during working memory, visual perception, visual attention and visual imagery [42,44,45,47,48,49,50,60,61]. In our study, the correlations between the deactivation of individual brain regions and task performance were not always significant, but almost all of the deactivated regions showed a trend of negative correlation with task performance (the more deactivated, the smaller the errors). Thus these regions could as a whole contribute significantly to the behavior but no region stands out as the "most significant" in our analysis.

Some of the regions that showed differential activity during perception and prediction (Table 2, Figure 3) were consistent with previous findings in the study of visual motion imagery, but there are also notable differences. Similar to previous studies, we observed greater activity during prediction, compared to perception, in the inferior parietal lobule (BA 40) [15], insula [14,15], and anterior cingulate [14]. On the other hand, greater activity in the lingual gyrus, the middle temporal gyrus and the inferrior frontal gyrus has not been reported in previous studies of visual motion imagery. The activation of the left superior parietal lobule, which has been reported in previous studies and has been implicated in the generation of mental images and in visual tracking tasks [12,16,17,18], was also not observed in our study. Our study also did not find the deactivation of sensory regions of other modalities, such as auditory and somatosensory cortex, which was shown in visual imagery in a previous study [48].

The observed differences between studies could reflect the effect of task variations in visual motion prediction and visual motion

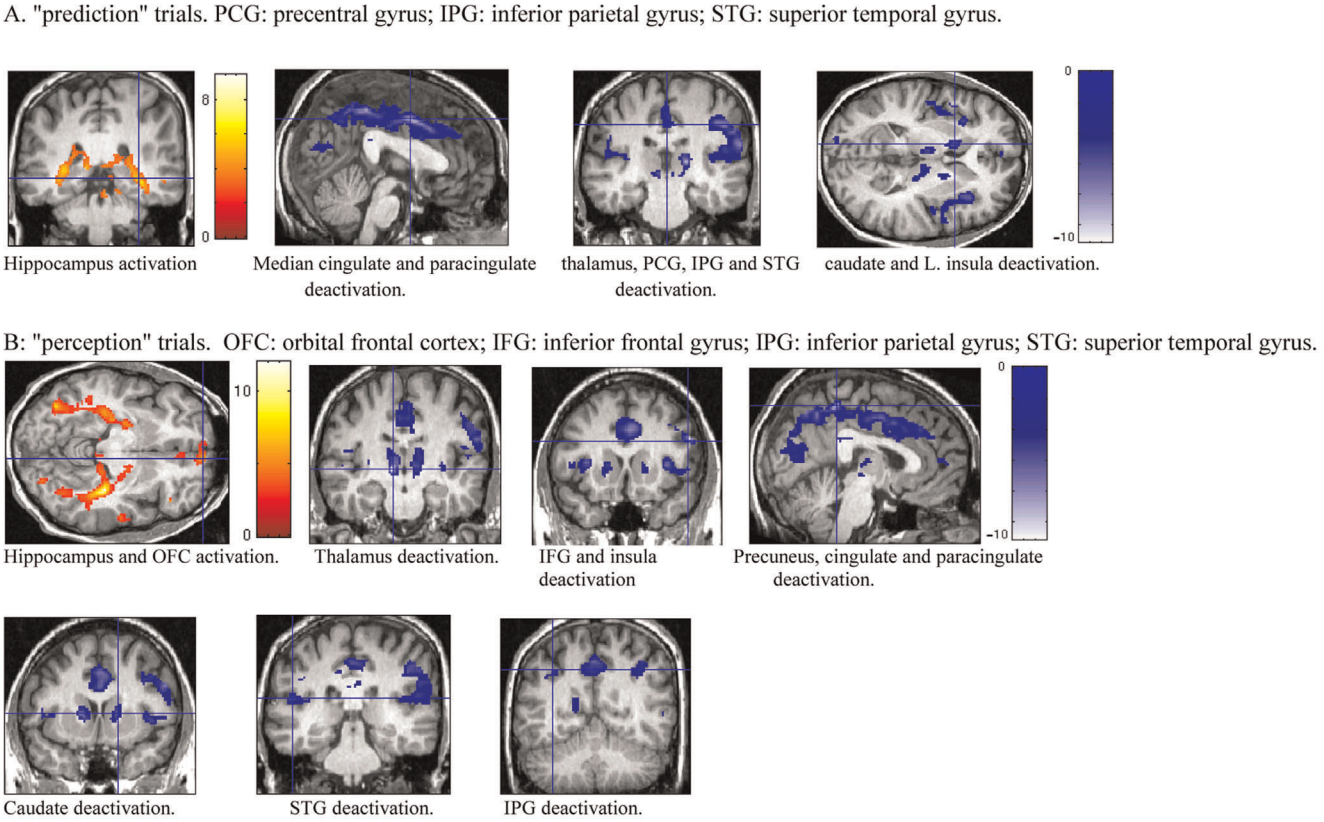

Figure 2. Regions of task-related activation and deactivation averaged over all subjects. A. "Prediction" trials. B. "Perception" trials. The warm colors indicate activation; and the cold colors indicate deactivation. The detailed description of each region is in Table 1.
doi:10.1371/journal.pone.0039854.g002

memory/imagery. Instead of recalling or imagining categorized motion (e.g. upward, downward, outward and inward) [3,14], subjects in our study had to accurately assess the initial motion of a moving object and then mentally update its changing location with time. Our event-related design is also unusual among studies of mental imagery and could contribute to observed differences in brain activity, such as reductions of activity with a slow time course (i.e. arousal and attention shifts). Our results indicate that visual

Table 2. Summary of differential brain activity during prediction and perception.

Region (BA)	Volumn (# voxels)	peak coord (x, y, z, MNI)	Peak T	p	% mod. Mean (ste)
Prediction - Perception:					
L. Insula	674	−36, 24, 8	9.69	<0.001	0.29 (0.03)
Anterior cingulate cortex (32)	808	6, 20, 42	7.83	<0.001	0.41 (0.08)
L. Inferior parietal gyrus (40)	183	−48, −42, 34	7.36	0.089	0.25 (0.04)
Lingual gyrus (30)	1532	−18, −66, 8	7.25	<0.001	0.30 (0.03)
R. Insula	542	44, 10, 2	7.15	<0.001	0.29 (0.05)
R. inferior parietal gyrus (40)	271	32, −54, 44	7.08	0.011	0.36 (0.07)
R. inferior frontal/precentral gyrus	350	48, 2, 34	6.25	0.002	0.29 (0.03)
L. middle temporal gyrus (39)	255	−52, −52, 6	5.44	0.016	0.35 (0.07)
Perception - Prediction:					
L. Middle occipital gyrus (18, 19)	507	−14, −98, 8	9.89	<0.001	0.42 (0.05)
R. middle occipital gyrus (18)	164	24, −96, 14	8.21	0.14	0.39 (0.09)
R. Middle occipital gyrus (19)	437	38, −82, −12	6.91	<0.001	0.38 (0.05)
R. cingulate gyrus	295	16, −16, 40	5.46	0.007	0.18 (0.03)

Peak coord: peak coordinates; p: corrected p value; % mod: % modulation.
doi:10.1371/journal.pone.0039854.t002

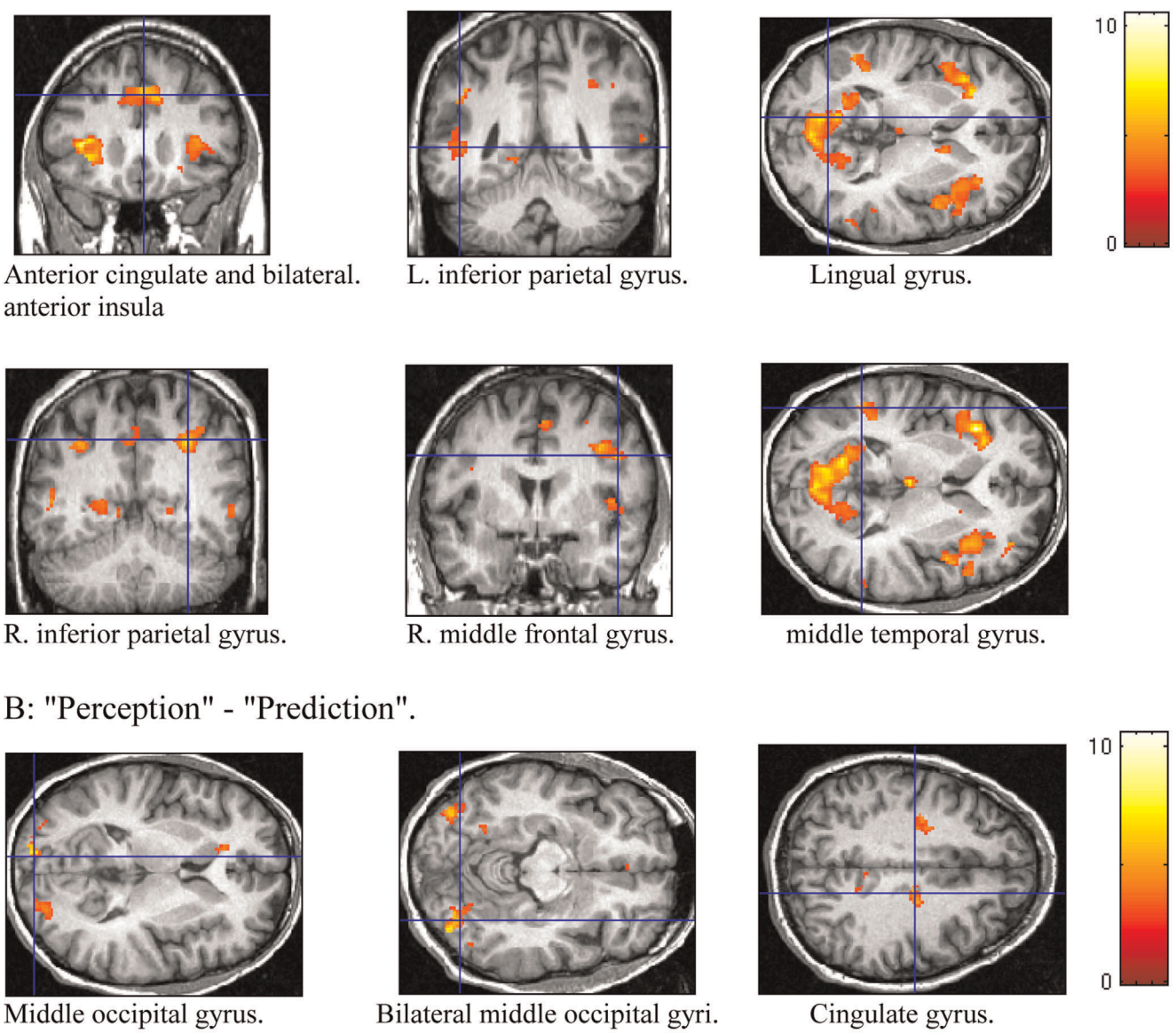

Figure 3. Contrast images averaged over all subjects. A. Prediction trials – Perception trials. B. Perception trials – Prediction trials. The detailed description of each region is in Table 2.
doi:10.1371/journal.pone.0039854.g003

motion trajectory prediction involves a different network of brain activity than visual motion perception and imagery, and further studies are needed to specifically examine the brain substrates of this behavior. Such differences also illustrate the complexity of studying the mechanisms of internally generated mental processes, and the difficulty of assessing whether subjects used identical cognitive strategies for different tasks.

A potential caveat of our study is that subjects could have used lapsed time to estimate the final location of the occluded object. We explicitly instructed the subjects not to use this strategy. Our variable trial time makes this strategy ineffective, in contrast to some previous designs [62]. The similar reaction times in perception and prediction trials also indicate that the lapsed time strategy was unlikely. If subjects used lapsed time to infer the travel distance, trajectory prediction would be expected to take much longer time than simple perception. Another caveat is that subjects may have used smooth eye pursuit to help tracking the invisible square as we did not track eye movements (except for one subject, whose eye tracking data did not show indications of smooth eye pursuit during the task). This is a common caveat in similar studies [11,14,63]. Several arguments make it unlikely that the brain activity that we observed was due mainly to smooth eye pursuit. First, if smooth eye pursuit took place, it would be similarly so in both "perception" and "prediction" trials and the differential brain activity that we observed should not be mainly due to eye movements. Second, we did not observe the activation of brain regions involved in smooth eye pursuit and eye movement, such as the supplementary eye field, the frontal eye field, brain stem and cerebellum [63,64,65]. Third, visual motion imagery studies that did record eye trace showed that subjects in general fixated well

Table 3. Correlations between regional brain activity and error rates.

Region (BA)	r (p, corrected)
Perception, Activation:	
R. hippocampus	0.09
L. hippocampus	−0.14
Orbital frontal	−0.45
Perception, Deactivation:	
L. Thalamus	−0.48
Inferior frontal	−0.74 (0.01)
Precuneus/m.cingulate/paracingulate	−0.75 (0.074)
R. Thalamus	−0.14
L. insula	−0.37 (0.071)
Caudate nucleus	−0.27 (0.10)
Superior temporal	0.01
Inferior parietal	−0.40
Prediction, Activation:	
R. hippocampus	0.10
L. hippocampus	0.11
Prediction, Deactivation:	
Median cingulate and paracingulate	−0.47
Precentral/inferior parietal	−0.62
R. Thalamus	−0.24
caudate	−0.25
Thalamus	−0.37
Insula	−0.57 (0.11)
Superior temporal	−0.15
Prediction – Perception:	
L. Middle occipital	0.45 (0.05)
R. middle occipital	0.49
L. Insula	−0.18
Anterior cingulate cortex	−0.35
L. Inferior parietal	−0.20
Lingual	−0.40
R. Insula	−0.59 (0.10)
R. inferior parietal	−0.01
R. inferior frontal	−0.15
L. middle temporal	−0.75 (0.08)
Perception – Prediction (with error in perception trials):	
R. Middle occipital	−0.05
R. cingulate	−0.43 (0.02)

Error rates during the prediction trials were used in this analysis, except when we calculated the correlation between error rates and the differential activity of "Perception" – "Prediction", in which case the error rates in perception trials were used.

doi:10.1371/journal.pone.0039854.t003

[15]. Another caveat, given that the prediction trials in our general linear model contained a brief period when the square was visible and a longer period when the square was occluded, is that the observed brain activity in the prediction trials was driven by the visible period. To control for this, we built an alternative model in which the prediction trials only included the occluded period. This model's imperfection lies in the fact that the brief visible period of the prediction trials now became part of the baseline and may obscure some brain activity. Indeed, we found that the brain activation in this model was weaker, so was the differential activity in "Prediction – Perception". However, the important point is that this "alternative" model revealed virtually the same brain regions activated and deactivated as in our main model. We are therefore confident that our main model was effective in the identification of brain regions involved in the motion prediction task.

The brain regions that showed greater activity during prediction trials have been implicated in a number of cognitive functions and are thought to be affected by healthy aging and by pathological states, such as depression and anxiety disorders, ADHD and the dementias. The ACC has been implicated as a crucial component of thoughts and actions. It has been implicated in conflict-monitoring, such as during the presentation of unexpected stimuli or conflicting information, or in the resolution of uncertainties [66,67,68,69]. The rostral ACC has also been associated with error checking and impulse control [70,71,72,73,74]. In our task, higher activity of the ACC in prediction trials is consistent with its functions in situations that involve response uncertainty and error checking. Hypoactivity of ACC has been observed during cognitive tasks in addicted individuals, nicotine users, and in ADHD [75,76,77,78]. ACC activity is also correlated with anger and aggression in healthy individuals [13] and is affected in normal aging [79]. The insular cortex, along with the ACC, has been proposed to form part of the "cognitive control network" or "salience network" and has been implicated in functions ranging from self-awareness and consciousness to decision-making, performance monitoring, time perception, sensory awareness, task switching and the detection of salient events [80,81]. The inferior parietal BA 40 has been implicated in working memory, executive control, motor planning and sensory functions [82,83], [84,85,86]. Particularly relevant to our task may be its role in spatial attention [87], visual processing [88], motion aftereffect [89], and auditory motion perception [90]. This region also shows altered activity in disorders such as ADHD, high risk for alcoholism and during aging [91,92,93].

It is expected that the motion responsive regions in the visual cortex are involved in the trajectory prediction. Because our scan was not conducted in a dark environment, subjects were able to see and were free to move their eyes during inter-trial intervals. This may be why we did not observe task-related activation of the visual cortex—our sparse visual stimuli (an FP and a very small moving square) may not have been a significant addition to the visual scene. Nonetheless, we observe greater activity of the extrastriate visual cortex in perception than in prediction trials. It is difficult, however, to interpret the correlation between such activity and error rates, because we do not know whether the activity arises from an activation of the visual cortex during perception, or a deactivation during prediction. Future studies with tightly controlled visual environment will be needed to address this issue.

Individuals with diminished sensory and cognitive abilities exhibit compromised performance in many tasks that involve motion trajectory prediction, such as driving, avoiding obstacles and reaching. For example, higher risks of traffic accidents are associated with aging, brain injury and some mental disorders (such as ADHD) [94,95,96,97,98,99]. Our results show that there is an extensive brain network that is involved in this behavior, and some of its components have been implicated in pathological processes. Further studies will need to determine specific contributions from these regions during motion trajectory prediction and how deficits in this process can impact daily mobility-related activity and can be affected by aging and mental disorders.

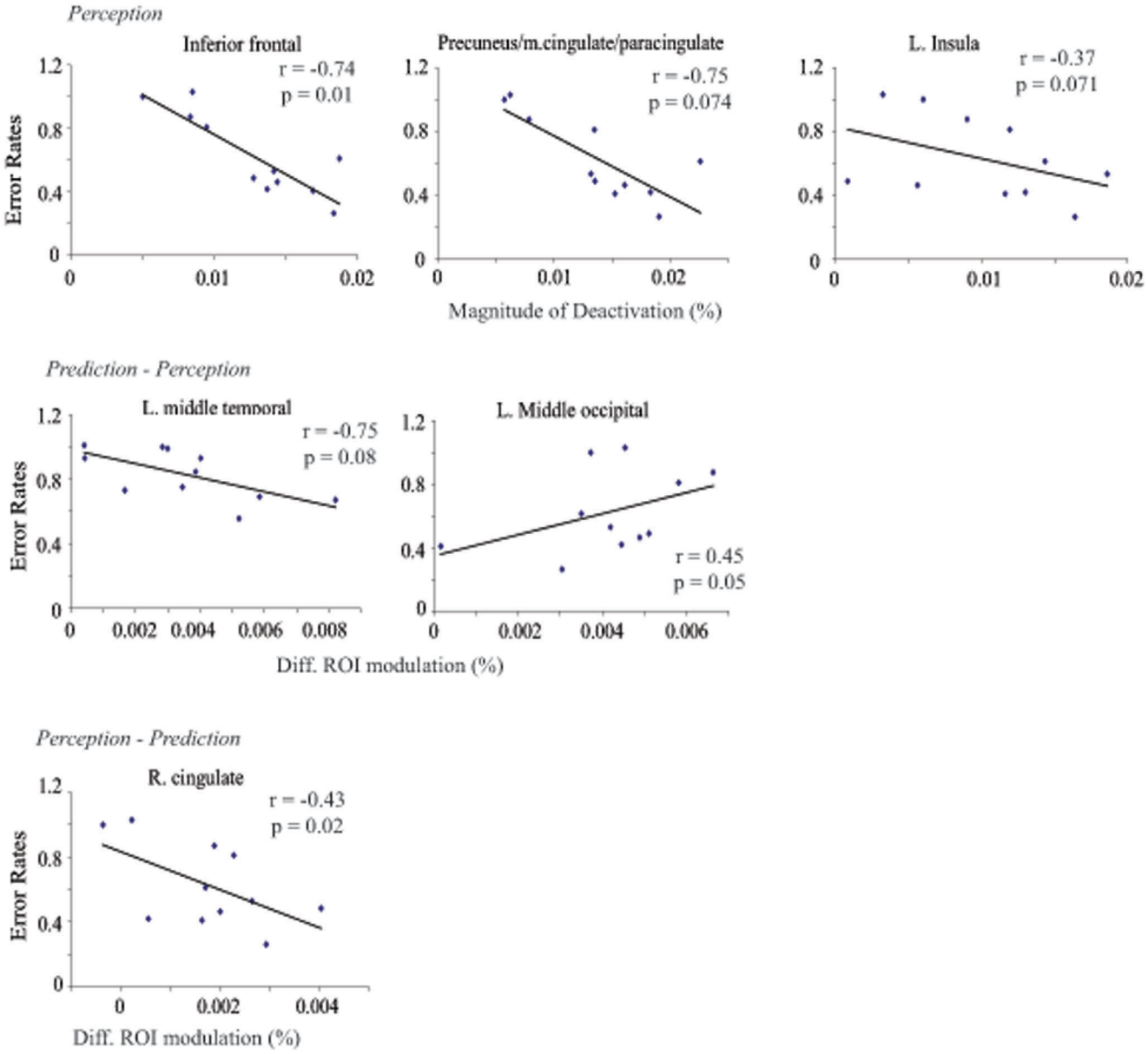

Figure 4. Scatter plots of the significant correlation between ROI modulation and error rates in prediction trials for all subjects. The complete list is in Table 3. Note that, for ROIs that showed task-related *deactivation*, the correlation is plotted between error rates and the *deactivation* level. In other words, the larger the number on the x axis, the larger the *deactivation*.
doi:10.1371/journal.pone.0039854.g004

Acknowledgments

We thank Heng Wang for technical assistance in data preparation and analysis, and Keith Neunham and Scott Peltier for assistance with fMRI data collection.

Author Contributions

Conceived and designed the experiments: JL. Performed the experiments: JL. Analyzed the data: DC JL. Contributed reagents/materials/analysis tools: JKZ. Wrote the paper: JL. Gave advice on study logistics, subject recruitment and general issues of human subject research: JKZ.

References

1. DeLucia PR, Mather RD (2006) Motion extrapolation of car-following scenes in younger and older drivers. Hum Factors 48: 666–674.
2. Umla-Runge K, Zimmer HD, Krick CM, Reith W (2011) fMRI correlates of working memory: Specific posterior representation sites for motion and position information. Brain Res 1382: 206–218.
3. Kawasaki M, Watanabe M, Okuda J, Sakagami M, Aihara K (2008) Human posterior parietal cortex maintains color, shape and motion in visual short-term memory. Brain Res 1213: 91–97.
4. Hussar CR, Pasternak T (2009) Flexibility of sensory representations in prefrontal cortex depends on cell type. Neuron 64: 730–743.
5. Zaksas D, Pasternak T (2006) Directional signals in the prefrontal cortex and in area MT during a working memory for visual motion task. J Neurosci 26: 11726–11742.
6. Anguera JA, Reuter-Lorenz PA, Willingham DT, Seidler RD (2010) Contributions of spatial working memory to visuomotor learning. J Cogn Neurosci 22: 1917–1930.

7. Podzebenko K, Egan GF, Watson JD (2002) Widespread dorsal stream activation during a parametric mental rotation task, revealed with functional magnetic resonance imaging. Neuroimage 15: 547–558.
8. Koshino H, Carpenter PA, Keller TA, Just MA (2005) Interactions between the dorsal and the ventral pathways in mental rotation: an fMRI study. Cogn Affect Behav Neurosci 5: 54–66.
9. Cohen MS, Kosslyn SM, Breiter HC, DiGirolamo GJ, Thompson WL, et al. (1996) Changes in cortical activity during mental rotation. A mapping study using functional MRI. Brain 119 (Pt 1): 89–100.
10. Pylyshyn ZW, Storm RW (1988) Tracking multiple independent targets: evidence for a parallel tracking mechanism. Spat Vis 3: 179–197.
11. Howe PD, Horowitz TS, Morocz IA, Wolfe J, Livingstone MS (2009) Using fMRI to distinguish components of the multiple object tracking task. J Vis 9: 10 11–11.
12. Culham JC, Cavanagh P, Kanwisher NG (2001) Attention response functions: characterizing brain areas using fMRI activation during parametric variations of attentional load. Neuron 32: 737–745.
13. Ishai A (2010) Seeing with the mind's eye: top-down, bottom-up, and conscious awareness. F1000 Biol Rep 2.
14. Goebel R, Khorram-Sefat D, Muckli L, Hacker H, Singer W (1998) The constructive nature of vision: direct evidence from functional magnetic resonance imaging studies of apparent motion and motion imagery. Eur J Neurosci 10: 1563–1573.
15. Kaas A, Weigelt S, Roebroeck A, Kohler A, Muckli L (2010) Imagery of a moving object: the role of occipital cortex and human MT/V5+. Neuroimage 49: 794–804.
16. Culham JC, Brandt SA, Cavanagh P, Kanwisher NG, Dale AM, et al. (1998) Cortical fMRI activation produced by attentive tracking of moving targets. J Neurophysiol 80: 2657–2670.
17. Sack AT, Camprodon JA, Pascual-Leone A, Goebel R (2005) The dynamics of interhemispheric compensatory processes in mental imagery. Science 308: 702–704.
18. Mechelli A, Price CJ, Friston KJ, Ishai A (2004) Where bottom-up meets top-down: neuronal interactions during perception and imagery. Cereb Cortex 14: 1256–1265.
19. Tootell RB, Mendola JD, Hadjikhani NK, Ledden PJ, Liu AK, et al. (1997) Functional analysis of V3A and related areas in human visual cortex. J Neurosci 17: 7060–7078.
20. Orban GA, Fize D, Peuskens H, Denys K, Nelissen K, et al. (2003) Similarities and differences in motion processing between the human and macaque brain: evidence from fMRI. Neuropsychologia 41: 1757–1768.
21. Britten KH (2003) The middle temporal area: motion processing and the link to perception. In: Chalupa LM, Werner JS, editors. Visual Neurosciences. 1 ed. Cambridge, MA: MIT Press.
22. Huk AC, Heeger DJ (2000) Task-related modulation of visual cortex. Journal of Neurophysiology 83: 3525–3536.
23. Smith AT, Greenlee MW, Singh KD, Kraemer FM, Hennig J (1998) The processing of first- and second-order motion in human visual cortex assessed by functional magnetic resonance imaging (fMRI). J Neurosci 18: 3816–3830.
24. Serences JT, Boynton GM (2007) The representation of behavioral choice for motion in human visual cortex. J Neurosci 27: 12893–12899.
25. McKeefry DJ, Burton MP, Vakrou C, Barrett BT, Morland AB (2008) Induced deficits in speed perception by transcranial magnetic stimulation of human cortical areas V5/MT+ and V3A. J Neurosci 28: 6848–6857.
26. Matthews N, Luber B, Qian N, Lisanby SH (2001) Transcranial magnetic stimulation differentially affects speed and direction judgments. Exp Brain Res 140: 397–406.
27. Beckers G, Zeki S (1995) The consequences of inactivating areas V1 and V5 on visual motion perception. Brain 118 (Pt 1): 49–60.
28. Beckers G, Homberg V (1992) Cerebral visual motion blindness: transitory akinetopsia induced by transcranial magnetic stimulation of human area V5. Proc Biol Sci 249: 173–178.
29. Cowey A, Campana G, Walsh V, Vaina LM (2006) The role of human extra-striate visual areas V5/MT and V2/V3 in the perception of the direction of global motion: a transcranial magnetic stimulation study. Exp Brain Res 171: 558–562.
30. Albright TD, Desimone R, Gross CG (1984) Columnar organization of directionally selective cells in visual area MT of the macaque. Journal of Neurophysiology 51: 16–31.
31. Liu J, Newsome WT (2003) Functional organization of speed tuned neurons in visual area MT. Journal of Neurophysiology 89: 246–256.
32. Liu J, Newsome WT (2005) Correlation between speed perception and neural activity in the middle temporal visual area. J Neurosci 25: 711–722.
33. Salzman CD, Murasugi CM, Britten KH, Newsome WT (1992) Microstimulation in visual area MT: effects on direction discrimination performance. The Journal of Neuroscience 12: 2331–2355.
34. Cheng K, Hasegawa T, Saleem KS, Tanaka K (1994) Comparison of neuronal selectivity for stimulus speed, length, and contrast in the prestriate visual cotical areas V4 and MT of the macaque monkey. Journal of Neurophysiology 71: 2269–2280.
35. Felleman DJ, van Essen DC (1987) Receptive field properties of neurons in area V3 of macaque monkey extrastriate cortex. Journal of Neurophysiology 57: 889–920.
36. Maunsell JHR, van Essen DC (1983) Functional properties of neurons in middle temporal visual area of the macaque monkey. I. Selectivity for stimulus direction, speed and orientation. Journal of Neurophysiology 49: 1127–1147.
37. Rodman HR, Albright TD (1987) Coding of visual stimulus velocity in area MT of the macaque. Vision Research 27: 2035–2048.
38. Bisley JW, Zaksas D, Droll JA, Pasternak T (2004) Activity of neurons in cortical area MT during a memory for motion task. J Neurophysiol 91: 286–300.
39. Bisley JW, Zaksas D, Pasternak T (2001) Microstimulation of cortical area MT affects performance on a visual working memory task. J Neurophysiol 85: 187–196.
40. Bisley JW, Pasternak T (2000) The multiple roles of visual cortical areas MT/MST in remembering the direction of visual motion. Cereb Cortex 10: 1053–1065.
41. Slotnick SD, Thakral PP (2011) Memory for motion and spatial location is mediated by contralateral and ipsilateral motion processing cortex. Neuroimage 55: 794–800.
42. Raichle ME, MacLeod AM, Snyder AZ, Powers WJ, Gusnard DA, et al. (2001) A default mode of brain function. Proc Natl Acad Sci U S A 98: 676–682.
43. Raichle ME, Snyder AZ (2007) A default mode of brain function: a brief history of an evolving idea. Neuroimage 37: 1083–1090; discussion 1097–1089.
44. Mayer JS, Roebroeck A, Maurer K, Linden DE (2010) Specialization in the default mode: Task-induced brain deactivations dissociate between visual working memory and attention. Hum Brain Mapp 31: 126–139.
45. Singh KD, Fawcett IP (2008) Transient and linearly graded deactivation of the human default-mode network by a visual detection task. Neuroimage 41: 100–112.
46. Daselaar SM, Porat Y, Huijbers W, Pennartz CM (2010) Modality-specific and modality-independent components of the human imagery system. Neuroimage 52: 677–685.
47. Mozolic JL, Joyner D, Hugenschmidt CE, Peiffer AM, Kraft RA, et al. (2008) Cross-modal deactivations during modality-specific selective attention. BMC Neurol 8: 35.
48. Amedi A, Malach R, Pascual-Leone A (2006) Negative BOLD differentiates visual imagery and perception. Neuron 48: 859–872.
49. Lewis JW, Beauchamp MS, DeYoe EA (2000) A comparison of visual and auditory motion processing in human cerebral cortex. Cereb Cortex 10: 873–888.
50. Laurienti PJ, Burdette JH, Wallace MT, Yen YF, Field AS, et al. (2002) Deactivation of sensory-specific cortex by cross-modal stimuli. J Cogn Neurosci 14: 420–429.
51. Glover GH, Law CS (2001) Spiral-in/out BOLD fMRI for increased SNR and reduced susceptibility artifacts. Magn Reson Med 46: 515–522.
52. Brett M, Anton JL, Valabregue R, Poline JB (2002) Region of interest analysis using an SPM toolbox. 8th International Conference on Functional Mapping of the Human Brain Sendai, Japan.
53. Zar JH (1999) Biostatistical analysis. New Jersey: Prentice Hall.
54. Chau W, McIntosh AR, Robinson SE, Schulz M, Pantev C (2004) Improving permutation test power for group analysis of spatially filtered MEG data. Neuroimage 23: 983–996.
55. Seiffert AE, Somers DC, Dale AM, Tootell RB (2003) Functional MRI studies of human visual motion perception: texture, luminance, attention and after-effects. Cereb Cortex 13: 340–349.
56. Hartley T, Maguire EA, Spiers HJ, Burgess N (2003) The well-worn route and the path less traveled: distinct neural bases of route following and wayfinding in humans. Neuron 37: 877–888.
57. Iaria G, Petrides M, Dagher A, Pike B, Bohbot VD (2003) Cognitive strategies dependent on the hippocampus and caudate nucleus in human navigation: variability and change with practice. J Neurosci 23: 5945–5952.
58. Maguire EA, Spiers HJ, Good CD, Hartley T, Frackowiak RS, et al. (2003) Navigation expertise and the human hippocampus: a structural brain imaging analysis. Hippocampus 13: 250–259.
59. O'Keefe J, Dostrovsky J (1971) The hippocampus as a spatial map. Preliminary evidence from unit activity in the freely-moving rat. Brain Res 34: 171–175.
60. Tomasi D, Ernst T, Caparelli EC, Chang L (2006) Common deactivation patterns during working memory and visual attention tasks: an intra-subject fMRI study at 4 Tesla. Hum Brain Mapp 27: 694–705.
61. McKiernan KA, Kaufman JN, Kucera-Thompson J, Binder JR (2003) A parametric manipulation of factors affecting task-induced deactivation in functional neuroimaging. J Cogn Neurosci 15: 394–408.
62. Benguigui N, Broderick M, Ripoll H (2004) Age differences in estimating arrival-time. Neurosci Lett 369: 197–202.
63. Schicke T, Muckli L, Beer AL, Wibral M, Singer W, et al. (2006) Tight covariation of BOLD signal changes and slow ERPs in the parietal cortex in a parametric spatial imagery task with haptic acquisition. Eur J Neurosci 23: 1910–1918.
64. Lencer R, Trillenberg P (2008) Neurophysiology and neuroanatomy of smooth pursuit in humans. Brain Cogn 68: 219–228.
65. Sweeney JA, Luna B, Keedy SK, McDowell JE, Clementz BA (2007) fMRI studies of eye movement control: investigating the interaction of cognitive and sensorimotor brain systems. Neuroimage 36 Suppl 2: T54–60.
66. Isomura Y, Takada M (2004) Neural mechanisms of versatile functions in primate anterior cingulate cortex. Reviews in the Neurosciences 15: 279–291.

67. Davidson MC, Horvitz JC, Tottenham N, Fossella JA, Watts R, et al. (2004) Differential cingulate and caudate activation following unexpected nonrewarding stimuli. Neuroimage 23: 1039–1045.
68. Liston C, Matalon S, Hare TA, Davidson MC, Casey BJ (2006) Anterior cingulate and posterior parietal cortices are sensitive to dissociable forms of conflict in a task-switching paradigm. Neuron 50: 643–653.
69. Yoshida W, Ishii S (2006) Resolution of uncertainty in prefrontal cortex. Neuron 50: 781–789.
70. Brown SM, Manuck SB, Flory JD, Hariri AR (2006) Neural basis of individual differences in impulsivity: contributions of corticolimbic circuits for behavioral arousal and control. Emotion 6: 239–245.
71. Menon V, Adleman NE, White CD, Glover GH, Reiss AL (2001) Error-related brain activation during a Go/NoGo response inhibition task. Human Brain Mapping 12: 131–143.
72. Kiehl KA, Liddle PF, Hopfinger JB (2000) Error processing and the rostral anterior cingulate: an event-related fMRI study. Psychophysiology 37: 216–223.
73. Casey BJ, Forman SD, Franzen P, Berkowitz A, Braver TS, et al. (2001) Sensitivity of prefrontal cortex to changes in target probability: a functional MRI study. Human Brain Mapping 13: 26–33.
74. Simmonds DJ, Pekar JJ, Mostofsky SH (2008) Meta-analysis of Go/No-go tasks demonstrating that fMRI activation associated with response inhibition is task-dependent. Neuropsychologia 46: 224–232.
75. Hester R, Nestor L, Garavan H (2009) Impaired error awareness and anterior cingulate cortex hypoactivity in chronic cannabis users. Neuropsychopharmacology 34: 2450–2458.
76. Goldstein RZ, Alia-Klein N, Tomasi D, Carrillo JH, Maloney T, et al. (2009) Anterior cingulate cortex hypoactivations to an emotionally salient task in cocaine addiction. Proc Natl Acad Sci U S A 106: 9453–9458.
77. Kaufman JN, Ross TJ, Stein EA, Garavan H (2003) Cingulate hypoactivity in cocaine users during a GO-NOGO task as revealed by event-related functional magnetic resonance imaging. J Neurosci 23: 7839–7843.
78. Bush G, Frazier JA, Rauch SL, Seidman LJ, Whalen PJ, et al. (1999) Anterior cingulate cortex dysfunction in attention-deficit/hyperactivity disorder revealed by fMRI and the Counting Stroop. Biol Psychiatry 45: 1542–1552.
79. Vaidya JG, Paradiso S, Boles Ponto LL, McCormick LM, Robinson RG (2007) Aging, grey matter, and blood flow in the anterior cingulate cortex. Neuroimage 37: 1346–1353.
80. Craig AD (2009) How do you feel–now? The anterior insula and human awareness. Nat Rev Neurosci 10: 59–70.
81. Menon V, Uddin LQ (2010) Saliency, switching, attention and control: a network model of insula function. Brain Struct Funct 214: 655–667.
82. Rama P, Martinkauppi S, Linnankoski I, Koivisto J, Aronen HJ, et al. (2001) Working memory of identification of emotional vocal expressions: an fMRI study. Neuroimage 13: 1090–1101.
83. Kirschen MP, Chen SH, Desmond JE (2010) Modality specific cerebro-cerebellar activations in verbal working memory: an fMRI study. Behav Neurol 23: 51–63.
84. Kubler A, Dixon V, Garavan H (2006) Automaticity and reestablishment of executive control-an fMRI study. J Cogn Neurosci 18: 1331–1342.
85. Fink GR, Marshall JC, Halligan PW, Frith CD, Driver J, et al. (1999) The neural consequences of conflict between intention and the senses. Brain 122 (Pt 3): 497–512.
86. Fincham JM, Carter CS, van Veen V, Stenger VA, Anderson JR (2002) Neural mechanisms of planning: a computational analysis using event-related fMRI. Proc Natl Acad Sci U S A 99: 3346–3351.
87. Thakral PP, Slotnick SD (2009) The role of parietal cortex during sustained visual spatial attention. Brain Res 1302: 157–166.
88. Lloyd D, Morrison I, Roberts N (2006) Role for human posterior parietal cortex in visual processing of aversive objects in peripersonal space. J Neurophysiol 95: 205–214.
89. Taylor JG, Schmitz N, Ziemons K, Grosse-Ruyken ML, Gruber O, et al. (2000) The network of brain areas involved in the motion aftereffect. Neuroimage 11: 257–270.
90. Lewald J, Staedtgen M, Sparing R, Meister IG (2011) Processing of auditory motion in inferior parietal lobule: evidence from transcranial magnetic stimulation. Neuropsychologia 49: 209–215.
91. Vance A, Silk TJ, Casey M, Rinehart NJ, Bradshaw JL, et al. (2007) Right parietal dysfunction in children with attention deficit hyperactivity disorder, combined type: a functional MRI study. Mol Psychiatry 12: 826–832, 793.
92. Rangaswamy M, Porjesz B, Ardekani BA, Choi SJ, Tanabe JL, et al. (2004) A functional MRI study of visual oddball: evidence for frontoparietal dysfunction in subjects at risk for alcoholism. Neuroimage 21: 329–339.
93. MacDonald SW, Nyberg L, Sandblom J, Fischer H, Backman L (2008) Increased response-time variability is associated with reduced inferior parietal activation during episodic recognition in aging. J Cogn Neurosci 20: 779–786.
94. Barkley RA, Cox D (2007) A review of driving risks and impairments associated with attention-deficit/hyperactivity disorder and the effects of stimulant medication on driving performance. J Safety Res 38: 113–128.
95. De Las Cuevas C, Sanz EJ (2008) Fitness to drive of psychiatric patients. Prim Care Companion J Clin Psychiatry 10: 384–390.
96. Edwards JD, Myers C, Ross LA, Roenker DL, Cissell GM, et al. (2009) The longitudinal impact of cognitive speed of processing training on driving mobility. Gerontologist 49: 485–494.
97. Park SW, Choi ES, Lim MH, Kim EJ, Hwang SI, et al. (2011) Association between unsafe driving performance and cognitive-perceptual dysfunction in older drivers. PM R 3: 198–203.
98. Richards E, Bennett PJ, Sekuler AB (2006) Age related differences in learning with the useful field of view. Vision Res 46: 4217–4231.
99. Jerome L, Segal A, Habinski L (2006) What we know about ADHD and driving risk: a literature review, meta-analysis and critique. J Can Acad Child Adolesc Psychiatry 15: 105–125.